Progress In Electromagnetics Research, Vol. 158, 63–72, 2017

Realization of All-Optical Digital Amplification in Coupled Nonlinear Photonic Crystal Waveguides

Vakhtang Jandieri[1, *], Ramaz Khomeriki[2], Daniel Erni[1], and Weng Cho Chew[3]

Abstract—In this conceptual study, all-optical amplification of the light pulses in two weakly coupled nonlinear photonic crystal waveguides (PCWs) is proposed. We consider two adjacent PCWs, which consist of line defects in a 2D square lattice of periodically distributed circular rods made from dielectric material with Kerr-type nonlinearity. Dispersion diagrams of the PCW's symmetric and antisymmetric modes are analyzed using a recently developed analytical formulation. The operating frequency is properly chosen to be located at the edge of the PCW's dispersion diagram (i.e., adjacent to the photonic crystals low-energy band edge), where in the linear case no propagation modes are excited. However, in case of a nonlinear medium when the amplitude of the injected signal is above some threshold value, solitons are formed propagating inside the coupled nonlinear PCWs. The near field distributions of the propagating light pulse inside the coupled nonlinear PCWs and the output power of the received signal are numerically studied in a detail. A very good agreement between the analytic soliton solution based on the nonlinear Schrödinger equation and numerical result is obtained. Amplification coefficients are calculated for the various amplitudes of the input signals. The results vividly demonstrate the effectiveness of the weakly coupled nonlinear PCWs as an all-optical digital amplifier.

1. INTRODUCTION

Photonic crystals (PhCs) have inspired a lot of interest due to their wide application for controlling of light within small length scales [1, 2]. PhCs are periodically modulated dielectric or metallic structures in which any electromagnetic wave propagation is forbidden within a fairly large frequency range (i.e., the photonic band-gap). Due to their dispersion, engineering features PhCs have enabled the implementation of linear functionalities into ultra-compact photonic devices, such as, e.g., acceleration or deceleration of propagating light fields, as well as their localization in the spatial and/or spectral domain. However, for the realization of true all-optical signal processing, the optical system needs to have nonlinear properties. In optically nonlinear media, the index of refraction is modified by the presence of a light signal and this modification can be exploited to influence another light signal, thereby performing an all-optical signal processing operation. Hence, PhCs are one of the most promising candidates to enable optical integration of many functions on the same chip leading to much lower production and operating costs.

In our recent papers, we have proposed a realistic model of an all-optical amplifier using either subwavelength metallic waveguides [3] or coupled linear PCWs [4]. Here, the effect of all-optical amplification is completely linear and there is no need for the implementation of nonlinear effects. However, the linear mechanism is based solely on superposition effects yielding therefore the

Received 7 January 2017, Accepted 24 March 2017, Scheduled 3 April 2017

* Corresponding author: Vakhtang Jandieri (vakhtang.jandieri@uni-due.de).

[1] General and Theoretical Electrical Engineering (ATE), Faculty of Engineering, University of Duisburg-Essen, and CENIDE — Center for Nanointegration Duisburg-Essen, D-47048 Duisburg, Germany. [2] Department of Physics, Tbilisi State University, 3 Chavchavadze, Tbilisi 0128, Republic of Georgia. [3] Electrical and Computer Engineering, 306 North Wright Street, Urbana, Illinois 61801, USA.

amplification of relative values regarding the input signal. Laser sources, on the other hand, provide sufficiently high light intensities to modify the optical properties of materials while enabling true interaction of light waves [5]. This scenario is investigated in the present manuscript, where two weakly coupled nonlinear PCWs are proposed as an efficient all-optical digital amplifier. The realization of all-optical digital amplifiers is demonstrated based on both analytical formulation and detailed numerical studies. We consider the coupled nonlinear rod-type PCWs, which is implemented into a 2D square lattice of the dielectric rods made from a pure Kerr-type material embedded in free space as the host medium. Soliton switching is successfully realized in such system [6] and one of the main advantages of the pillar type PCW is that it supports one even symmetry mode, which allows for an effective single mode operation. Although pure Kerr medium could be found in a variety of materials, it is obvious that from an application point of view, it would be better to consider more realistic PhCs structures, such as, e.g., the planar hole-type PhC with a nonlinear silicon background material (or, e.g., a nonlinear polymer hole filling). Planar silicon PCWs are promising candidates for the successful realization of various nonlinear optical devices on a chip [7–10]. Although nonlinear effects are greatly enhanced in silicon, they are not only of Kerr type, which highly complicates analytical considerations. In this conceptual study of all-optical amplification, we therefore examine the slightly idealized pillar-type dielectric PCWs. Light amplification in air-hole type nonlinear silicon PCWs encompasses a further investigative step aiming at the realization of all-optical digital amplifiers and logic gates for future photonic circuits.

The underlying idea of digital all-optical amplification is based on the phenomenon of band-gap transmission [11–15] in periodic nonlinear media [16, 17]. This effect takes place when the frequency of the injected signal is very close to the band edge of the PhC. In the linear case no transmission occurs. However, in the nonlinear case above some threshold value of the signal amplitude, the propagation of solitons takes place as associated eigen-solutions of the specific nonlinear setting. Such a bifurcation could be observed in both spatial and temporal domains [18, 19]. Particularly, in waveguide arrays [20, 21] one can observe band-gap transmission of self-focusing beams [22], while in optically active media [23] and Bragg gratings [24–27], temporal solitons are created. In principle, the latter two systems could be used for all optical signal amplification too, but they do not guarantee a good confinement of the light in the slow light regime, which is a necessary condition for the enhancement of the nonlinear effects [28]. Therefore, we are focusing on PCWs, where light confinement is inherently present and moreover, the structure is characterized by relatively small intrinsic losses. The amplification coefficient is calculated for different amplitudes of the input signal and the applicability as well as the efficiency of the weakly coupled nonlinear PCWs as all-optical digital amplifier is vividly demonstrated. We believe that these studies provide a practical methodology for designing ultra-compact nonlinear optical devices applicable to future all-optical computing systems.

2. FORMULATION OF THE PROBLEM

The effect of all-optical amplification is analyzed based on two adjacent weakly coupled PCWs each consisting of a line defect (i.e., a $W1$ waveguide) within a square lattice PhC. The geometry of the problem is illustrated in Fig. 1. Hence, the guiding regions are bounded by an upper and lower PhC slab having a thickness of N periods with h as the period of the PhC. The width of each waveguide is $w = 2h$ in case of a $W1$ waveguide. All rods are made of a Kerr-type dielectric material and the radius of the rods is r. There exist TE and TM (super-) modes in the two-dimensional coupled PCWs. Here we consider TE modes only having the following electric and magnetic field components (E_y, H_x, H_z). The TM modes consist of the field components (H_y, E_x, E_z) and can be treated in the same way.

For a proper analysis we start with the nonlinear Maxwell's equations, which are written in the following form:

$$\begin{aligned} &\frac{\partial E_y}{\partial z} = -\mu_0 \frac{\partial H_x}{\partial t}, \frac{\partial E_y}{\partial x} = \mu_0 \frac{\partial H_z}{\partial t} \\ &\frac{\partial H_z}{\partial x} - \frac{\partial H_x}{\partial z} = \varepsilon_0 \frac{\partial}{\partial t}\left[n^2 E_y + \chi^{(3)} E_y^3\right] \end{aligned} \tag{1}$$

where ε_0 and μ_0 are the permittivity and permeability of the free space, respectively. We introduce the spatially varying index of refraction $n(x, z)$, which we assume to be purely real neglecting any extinction

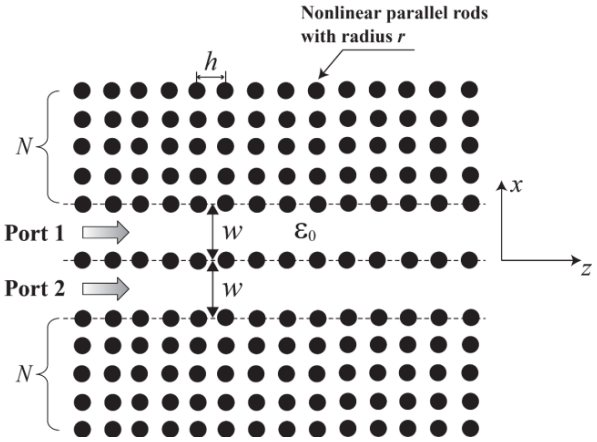

Figure 1. Schematic view of the symmetric coupled nonlinear PCWs embedded in a square lattice PhC made of dielectric rods in air as host medium, where h is the period of the PhC and $w = 2h$ is the width of each of the coupled $W1$ defect waveguide. The rods are parallel to the y-axis and made of a Kerr-type dielectric material. The size of the upper and lower PhC slab is denoted by N. The signals are launched into the coupled PCWs through Port 1 and Port 2.

due to absorption. The quantity $\chi^{(3)}$ stands for the third-order nonlinear optical susceptibility, which is related to the nonlinear refractive index n_2 through the following expression: $\chi^{(3)} = \frac{4}{3}n^2 n_2 \varepsilon_0 c$, where c is the speed of light.

Recently, Yasumoto and Jandieri have developed a self-consistent coupled-mode formulation for the coupled PCWs using perturbation theory (assuming small perturbations in the mode propagation constant) [29, 30]. It provides both a useful analytical technique for the approximation of the coupling between adjacent PCWs and a good physical insight of the underlying coupling mechanisms. In the first-order coupled-mode analysis, the guided field supported by the two-parallel waveguide system is approximated using the Floquet theorem as follows [29, 30]:

$$E_y(x, z, t) = F(t, z - vt)\Phi(x, z)e^{i(\beta z - \omega_0 t)} + c.c. \tag{2}$$

where β is a propagation constant along the z-axis, $\omega_0(\beta)$ corresponds to the frequency of the fundamental symmetric $\omega_S(\beta)$ or antisymmetric $\omega_A(\beta)$ (super-) modes of the coupled PCWs, $\Phi(x, z)$ denotes the (super-) mode's transverse field distribution supporting following symmetric $\Phi_S(-x, z) = \Phi_S(x, z)$ and anti-symmetric $\Phi_A(-x, z) = -\Phi_A(x, z)$ properties with respect to the x-axis and having a periodicity in z with a period $2\pi/h$ [29, 30]. The function $F(t, z - vt)$ depicts the slowly-varying amplitude and $v_{S,A}$ denotes a group velocity for symmetric and antisymmetric (super-) modes, respectively. Please note that the indices "S" and "A" stand for "symmetric" and "antisymmetric", respectively, and the notion "super-mode" is abbreviated to "mode" for simplicity reasons. The evolution of the slowly varying envelope characterizing the amplitude $F_{S,A}(t, z - vt)$ of the electric field pulse for the symmetric and antisymmetric modes with the change of variables to a moving frame $\xi = z - v_{S,A}t$ satisfies the nonlinear Schrödinger equation:

$$2i\frac{\partial F_{S,A}}{\partial t} + \omega''_{S,A}\frac{\partial^2 F_{S,A}}{\partial \xi^2} + \gamma F_{S,A}\left|F_{S,A}\right|^2 = 0 \tag{3}$$

where $\omega''_{S,A} = \frac{\partial^2 \omega_{S,A}}{\partial \beta^2}$. From Eq. (3) we can derive the soliton solution written in the following form [31]:

$$F_{S,A}(z, t) = \frac{F^0_{S,A}\exp(i\,\delta\omega_{S,A}t)}{\cosh\left[(z - v_{S,A}t)/\Lambda_{S,A}\right]} \tag{4}$$

with

$$\Lambda_{S,A} = \frac{1}{F^0_{S,A}}\sqrt{\frac{2\omega''_{S,A}}{\gamma}}, \quad \delta\omega_{S,A} = \frac{1}{4}\gamma\left(F^0_{S,A}\right)^2 \tag{5}$$

where $\Lambda_{S,A}$ is a temporal soliton width (FWHM) having symmetric or antisymmetric properties, $\delta\omega_{S,A}$ denotes the phase shift of the localized modes due to the nonlinearity of the rods, $F^0_{S,A}$ are soliton amplitudes, and the coefficient of nonlinearity is equal to $\gamma = 3\omega_{S,A}\chi^{(3)}\kappa/4$, where $\chi^{(3)}$ includes an enhancement effect due to the pulse slowdown in the coupled PCWs [28]. Note that in the homogeneous nonlinear medium $\kappa = 1$, whereas in case of inhomogeneous nonlinear medium such as the coupled PCWs within the nonlinear rod-type PhC (Fig. 1) κ can be defined from the definition of the nonlinear contribution regarding the electromagnetic field energy:

$$\kappa = \int\limits_{\Gamma'} |\Phi(x,z)|^4 \, dxdz \Big/ \int\limits_{\Gamma} |\Phi(x,z)|^4 \, dxdz \tag{6}$$

where Γ' encompasses only the area of the nonlinear dielectric rods and Γ the whole area of the coupled PCW's supercell. Given the proper geometry of the coupled PCWs, we can calculate the nondimensional parameter κ by studying supercell of the PCWs. When the value of κ, which is related to the nonlinear coefficient γ, is found, the analytic soliton solution based on the Eqs. (4) and (5) is directly obtained. For a proper validation the achieved analytic soliton solution is compared in Section III to a full-wave computational electromagnetics analysis.

The principle of all-optical amplification in the coupled nonlinear PCW is as follows: first, we properly choose the operating frequency ω located at the edge of the dispersion curve where no propagating modes are excited. Without loss of generality, let us assume that the operating frequency ω is located very close to the frequency at which only the antisymmetric propagating mode is excited in the coupled PCWs (see red circle in Fig. 2). In this case, Eqs. (4) and (5) together with (2) reveals that the operating frequency ω is given as follows:

$$\omega(\beta) = \omega_A(\beta) - \gamma \left(F^0_A\right)^2 \Big/ 4 \tag{7}$$

Now we launch a signal at this particular frequency in Port 1 of the coupled PCWs, whereas no signal is injected into Port 2 (see Fig. 1). The input signal can be considered as a linear combination of the symmetric and antisymmetric modes having the same amplitudes. Due to the fact that neither symmetric nor antisymmetric propagating modes are excited at this particular frequency (both of the modes are evanescent), there is no propagating signal inside the coupled nonlinear PCWs and hence, no output power. Now, additionally a signal with a small amplitude δ is injected through Port 2 into the guiding structure. Since we are dealing with weakly coupled PCWs, the total signal in the coupled PCWs could be presented as a linear combination of the symmetric and antisymmetric modes with

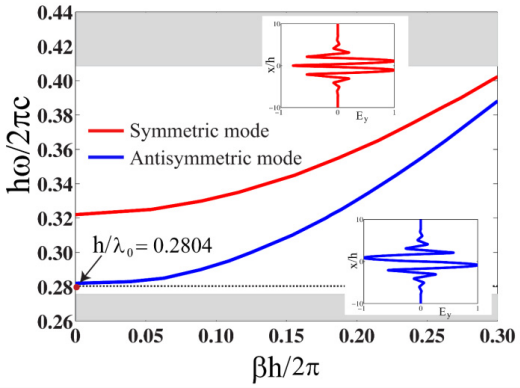

Figure 2. Dispersion curves of the symmetric (red line) and the antisymmetric (blue line) (super) modes of the coupled PCWs as shown in Fig. 1, where $r = 0.2h$, $n_0 = 3.4$ and $w = 2.0h$. The length of the photonic crystals is $50h$. The photonic bandgap of the underlying PhC lies in the range $0.277 < h\omega/2\pi c < 0.410$ in terms of normalized frequencies. The operation frequency is $h\omega/2\pi c = 0.2804$ marked by the red dot. The distributions of the electric field E_y for the symmetric and antisymmetric modes are presented within the corresponding insets.

different amplitudes: $(1-\delta)/2$ for the antisymmetric mode and $(1+\delta)/2$ for the symmetric mode [4]. The increased power inside the coupled PCWs due to the additional signal in Port 2 causes the frequency shift due to the Kerr-type nonlinearity of the rods $\gamma \neq 0$ [as it follows from Eq. (7)] yielding an operation point that allows the excitation of the antisymmetric propagating mode (see Fig. 2). Note that the symmetric mode remains evanescent. As a result, the electric fields of the propagating antisymmetric mode $E_y^A(x,z,t)$ and that of the evanescent symmetric mode $E_y^S(x,z,t)$ are expressed as:

$$E_y^A = \Phi_A(x,z)\frac{F_A^0 \exp[i(\beta_A z - \omega t)]}{\cosh\left[F_A^0(z-v_A t)\sqrt{\gamma/2\omega''}\right]} + c.c. \tag{8}$$

$$E_y^S = \Phi_S(x,z)\, F_S^0 \exp(-i\omega t - |\beta_S| z) + c.c. \tag{9}$$

In the limit of a weak nonlinearity and at large relative group velocities of the modes, the solutions (8) and (9) can be combined and the mechanism can be interpreted as a nonlinear "superposition" of propagating and evanescent modes [32]. Finally, the amplification coefficient (i.e., power gain g) in the coupled nonlinear PCWs is defined as the ratio of the total output power of Port 1 and Port 2 over the power of the signal injected into Port 2.

3. NUMERICAL RESULTS AND DISCUSSIONS

In order to verify the applicability of the coupled nonlinear PCWs as all-optical digital amplifier, we numerically study the two weakly coupled symmetric PCWs illustrated in Fig. 1. The thickness of the two PhC slabs is $N = 10$ with a period h. The radius of the rod is $r = 0.2h$, its linear refractive index is $n = 3.4$ and the injected peak power is chosen as $\chi^{(3)}[E_y^0]^2 = 6.5$, where E_y^0 is the electric field amplitude of the signal launched into Port 1 of the coupled PCW. The width of each $W1$ waveguide forming the PCW is $w = 2.0h$ and the length of the PhC is $50h$. In case of PhC defect waveguiding, the modes are confined in the guiding region only due to the existence of the photonic band-gap. Under the adjusted parameters, the rod-type PhC has photonic bandgap for the TE mode (E_y, H_x, H_z) covering the frequency range of $0.277 < h\omega/2\pi c < 0.410$. The dispersion diagrams of the coupled PCWs (Fig. 1) are studied based on the coupled-mode formulation [29, 30], which we have recently proposed using the first-order perturbation theory while taking into account a weak coupling effect (mutual coupling coefficient is much smaller than the propagation constant in the single isolated PCW). Based on the derived coupled-mode equations the propagation constant $\beta h/2\pi$ of the weakly coupled PCWs (Fig. 1) for both the symmetric mode and antisymmetric mode versus the normalized frequency $h\omega/2\pi c$ is calculated and plotted in Fig. 2 by a red and a blue line, respectively. The distributions of the electric field E_y for the symmetric and antisymmetric modes in the cross-section plane $z = 0$ at $h\omega/2\pi c = 0.33$ are also presented as corresponding insets in Fig. 2. We can see that the fields of the modes in the coupled PCWs are well confined in the guiding region. We have plotted the distributions of the electric field E_y in order to give a general picture about the confinement of the modes in the coupled PCWs. Based on our studies, no noticeable changes of the shape of the modes are observed by changing the excitation frequency. It is worth mentioning that no other propagating mode exists in the frequency range $0.277 < h\omega/2\pi c < 0.410$. Moreover, the structure shown in Fig. 1 is characterized by its relatively small intrinsic losses, which makes it a promising candidate for moving beyond the conceptual analysis of an all-optical digital amplifier towards a realistic case that will be supported by corresponding measurements.

All the numerical analyses that follow are conducted at the fixed normalized frequency $h\omega/2\pi c = 0.2804$ marked by the red dot in Fig. 2. It should be emphasized that it is located at the edge of the dispersion curve of the antisymmetric mode (blue line) very near to $h\omega_A(\beta = 0)/2\pi c$ where no propagating modes are excited at this frequency for small input amplitudes. First, a continuous signal with unit amplitude and at the normalized frequency $h\omega/2\pi c = 0.2804$ is launched into the upper PCW through Port 1, whereas no signal $\delta = 0$ is launched in Port 2. The signal is excited by a point source. Note that δ denotes the amplitude of the signal launched in the lower PCW through Port 2. Numerical analyses are conducted based on the FDTD method using the Berenger's PML to confine the simulation domain [8, 33]. Figs. 3(a)–3(d) depict the near field distributions of the signal propagating inside the coupled nonlinear PCWs at different time steps. The output signal is registered at a distance $z = 30h$

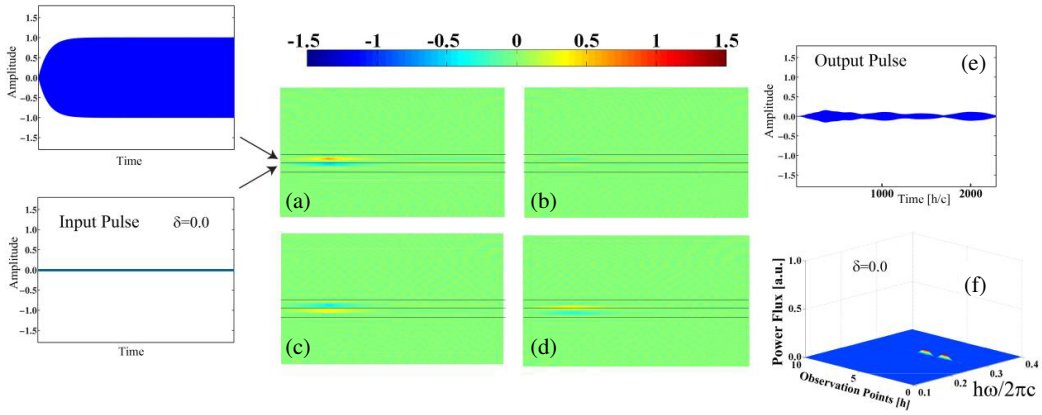

Figure 3. (a)–(d): Near field distributions of the signal propagation inside the coupled nonlinear PCWs (Fig. 1) at different time steps, when a continuous input signal is launched through Port 1 and no input signal $\delta = 0$ is injected in Port 2. (e): Amplitude of the electric field of the received signal at a distance $z = 30h$ inside the coupled PCWs. (f): Energy flux density of the output signal at a distance $z = 30h$ inside the coupled nonlinear PCWs. The boundaries of PCWs are marked by thin black lines.

inside the coupled PCWs. The amplitude of the electric field E_y and the energy flux density (i.e., Poynting field) of the output signal at $z = 30h$ are shown in Figs. 3(e) and 3(f), respectively. From Fig. 3 follows that the signal is not propagating inside the coupled nonlinear PCWs since both modes are evanescent and the received output power is negligibly small at $h\omega/2\pi c = 0.2804$.

Next, in order to demonstrate the coupled nonlinear PCWs (Fig. 1) capability as an all-optical digital amplifier, we additionally inject a Gaussian pulse in Port 2 with an amplitude $\delta = 0.5$ and the same normalized frequency $h\omega/2\pi c = 0.2804$. It should be emphasized that in order to guide an input signal into the coupled PCWs, which supports only one antisymmetric mode marked by blue line in the dispersion diagram (Fig. 2), the injected signals in Port 1 and Port 2 should be launched with opposite phases (the signals with the same phases will be completely reflected from the coupled PCWs [4]). An increased input power compared to Fig. 3 causes the dispersion $\omega\,(\beta)$ to shift to lower frequencies because of the Kerr-type nonlinearity leading again to an operation point that allows for a propagating antisymmetric mode (the symmetric mode is evanescent) that carries a soliton inside the PCWs as shown in Figs. 4(a)–4(d). It is worth emphasizing that in case of PCWs in a rod-type PhC the frequency shift is very small, since the modes are strongly confined in the $W1$ waveguide channel (Fig. 2). Only a small fraction of the field interacts with the rods yielding a minor change of the nonlinear refractive index n_2 of the rods. This fact is mainly reproduced by the nondimensional parameter κ given by Eq. (6). Under the prescribed geometrical conditions and in case of the antisymmetric mode, its value is estimated to be $\kappa \approx 0.01$. Fig. 4(e) shows a very good agreement between the analytic soliton solution (dotted red line) and the numerical result. This agreement should be considered as an important result showing that the analytical nonlinear Schrödinger model is capable of significantly increase the credibility of the numerical analysis.

The numerical analysis has also shown that the nonlinear PCWs (Fig. 1) is supporting slow light propagation with a group velocity $c/13$ (where the denominator represents the slowdown factor) [28]. When a pulse undergoes slow wave propagation, it will be significantly compressed, which in turn increases the peak intensity of the electric field [cf. Fig. 4(e)]. Its enhancement is accounted for by multiplying $\chi^{(3)}$ with the square of the slowdown factor (in our case slowdown factor is equal to 13). The output energy flux density at $\delta = 0.5$ is also presented in Fig. 4(f). The amplification coefficient g, which is calculated as a ratio of the total output power of Port 1 and Port 2 over the input power launched through Port 2 amounts to a power gain of $g = 3.1$. Similar numerical analyses as in Fig. 4 are conducted for an amplitude $\delta = 0.18$ of the injected signal in Port 2. The results are displayed in Fig. 5. Numerical studies have shown that the amplification coefficient (i.e., power gain) g increases inversely proportional to the amplitude δ and it is equal to $g = 9.5$ at $\delta = 0.18$. Our analysis underpins the applicability and effectiveness of the coupled nonlinear PCWs as an all-optical digital amplifier.

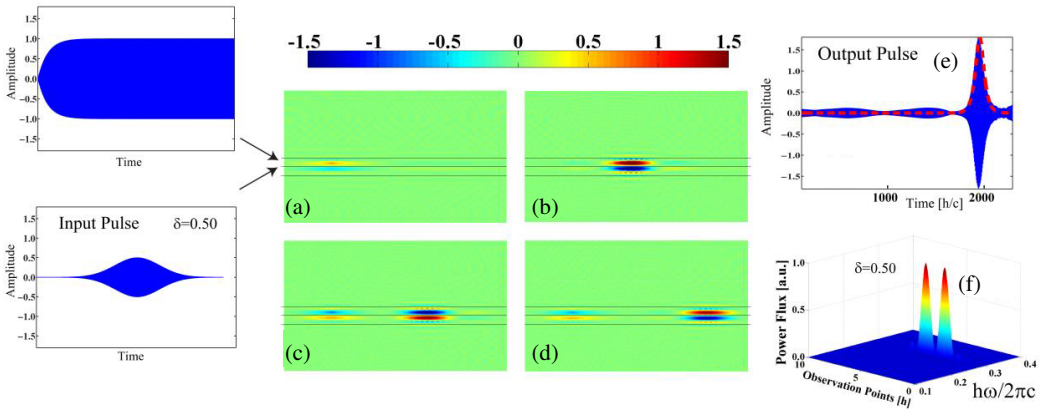

Figure 4. (a)–(d): Near field distributions of the signal propagation inside the coupled nonlinear PCWs (Fig. 1) at different time steps, when a continuous input signal is launched through Port 1 and Gaussian pulse with an amplitude $\delta = 0.5$ is injected in Port 2. (e): Amplitude of the electric field of the received signal at a distance $z = 30h$ inside the coupled PCWs. The dashed red line represents the result obtained analytically based on the Eqs. (4)–(6). (f): Power flux of the output signal at a distance $z = 30h$ inside the coupled nonlinear PCWs.

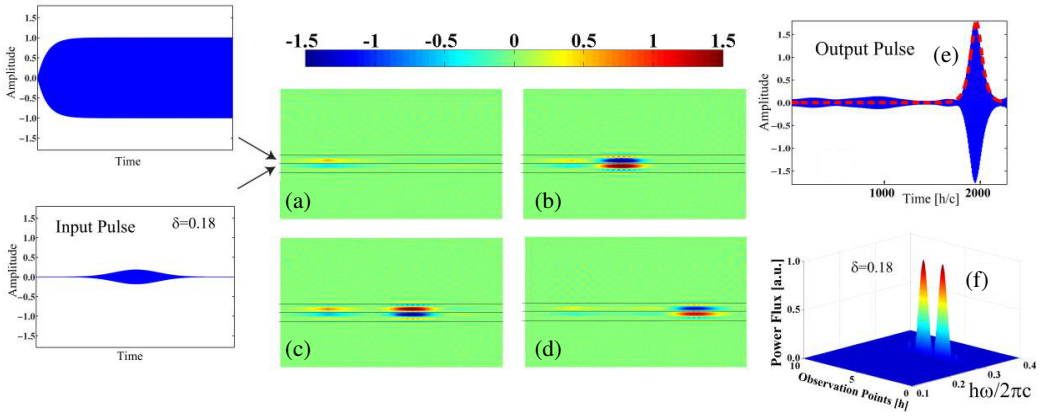

Figure 5. The same scenario as in Fig. 4, but for $\delta = 0.18$.

Very interesting point worth mentioning is that the total output energy flux density of the signal registered inside the coupled nonlinear PCW does not depend on the input power launched in Port 2. This phenomenon has been investigated for much simpler case [12] when a train of solitons with definite shape and amplitude is created when continuous signal amplitude exceeds the threshold. If continuous signal amplitude is below the threshold, no soliton is generated. The weak signal injected into port 2 helps thus to overcome the amplitude threshold at certain moment and soliton can be generated with amplitude and shape completely defined by continuous signal injected into Port 1. In other words, a weak signal triggers the creation of the soliton not influencing much its shape and power. This effect could be observed when comparing the output energy flux density in Fig. 4(f) (at $\delta = 0.5$) and Fig. 5(f) (at $\delta = 0.18$), respectively. It should be noted that we have calculated the total output energy flux density for various amplitudes δ of the signal injected in Port 2. The results reproduce the same profiles as those observed in Fig. 4(f) (at $\delta = 0.5$) and Fig. 5(f) (at $\delta = 0.18$). This is a unique feature of the coupled nonlinear PCWs that will never emerge in the linear case.

In this conceptual numerical study using coupled PCWs embedded into a nonlinear rod-type PhCs, the modulation of the nonlinearity is relatively weak due to a marginal overlap of the mode field with the Kerr medium. The rod-type PhC was chosen because the $W1$ PCWs support an easily achievable single mode operation. However, it should be noted that the PCWs embedded in a square lattice PhC

made of dielectric rods is impractical for experiments. Nevertheless, the chosen setting still allowed us to convincingly demonstrate — actually for the first time — the effect of all-optical amplification in weakly coupled PCWs based on the principle of band-gap transmission. It is now easier to transfer the proposed idea to PCWs that are embedded in more realistic PhC structures, such as, e.g., the hole-type PhC with a nonlinear background material (or nonlinear hole fillings). Travelling light amplification in air-hole type nonlinear PCWs is now under our intensive investigation aiming at the realization of all-optical logic gates for future photonic circuits. Another application could be plasmonic waveguide, however the fabrication of the effective plasmonic devices is still quite difficult because of a high loss.

4. CONCLUSION

In this conceptual study, we have proposed for the first time weakly coupled nonlinear PCWs as a realistic model for a functional all-optical digital amplifier. Deep physical insight is provided to the all-optical amplification effect of light pulse in the coupled nonlinear PCWs in the framework of the nonlinear Schrödinger equation. This is underpinned by the perfect agreement between the corresponding numerical examples and the theoretical analysis. The amplification coefficient (i.e., power gain) has been calculated for the various amplitudes of the input signals that have been launched into the coupled nonlinear PCWs. The results have demonstrated the effectiveness of the proposed structures as all-optical digital amplifier. Being capable of precisely control one light beam using another mimics the working principle of an optical transistor that is apt for performing complex light-control in all-optical circuits. Hence, we believe that one of the most promising practical applications of the proposed PCW structure are optical transistors, which forms the backbone of all-optical computing. One additional point of worth noticing is that in order to realize the all-optical amplification effect based on the proposed idea, the signal-to-noise ratio should be high.

Finally, it is worth looking at the coupling strength between the PCWs from the viewpoint of their application as all-optical amplifiers. Our studies are based on the weak coupling approximation. Assuming weak coupling allowed us to solve Maxwell's equations yielding analytical expressions for the evolution of the slowly varying envelope of the field that satisfies the nonlinear Schrödinger equation. We could give physical insight into the principle of all-optical amplification in the coupled nonlinear PCWs. However, we should mention that the principle of all-optical amplification could be realized even for relatively strong coupling between PCWs, which has already been proven in the framework of ongoing numerical simulations aiming at realistic planar PhC devices.

ACKNOWLEDGMENT

V. Jandieri acknowledges financial support from Alexander von Humboldt Foundation. The work is supported by Shota Rustaveli National Science Foundation (SRNSF) under Grant No. 216662 and Grant No. FR/25/6-100/14. D. Erni acknowledges the support from the DFG SFB/TRR 196 MARIE.

REFERENCES

1. Yablonovitch, E., "Inhibited spontaneous emission in solid-state physics and electronics," *Phys. Rev. Lett.*, Vol. 58, 2059–2062, 1987.
2. John, S., "Strong localization of photons in certain disordered dielectric superlattices," *Phys. Rev. Lett.*, Vol. 58, 2486–2489, 1987.
3. Khomeriki, R. and J. Leon, "All-optical amplification in metallic subwavelength linear waveguides," *Phys. Rev. A*, Vol. 87, 053806–053809, 2013.
4. Jandieri, V. and R. Khomeriki, "Linear amplification of optical signal in coupled photonic crystal waveguides," *IEEE Photonics Technology Letters*, Vol. 27, 639–641, 2015.
5. Malaguti, S., G. Bellanca, S. Combrie, A. de Rossi, and S. Trillo, "Temporal gap solitons and all-optical control of group delay in line-defect waveguides," *Phys. Rev. Lett.*, Vol. 109, 163902, 2012.

6. Cuesta-Soto, F., A. Martínez, J. García, F. Ramos, P. Sanchis, J. Blasco, and J. Martí, "All-optical switching structure based on a photonic crystal directional coupler," *Optics Express*, Vol. 12, 161–167, 2004.
7. Adibi, A., Y. Xu, R. Lee, A. Yariv, and A. Scherer, "Properties of the slab modes in photonic crystal optical waveguides," *J. Lightwave Technology*, Vol. 18, 1554–1564, 2000.
8. Qiu, M., K. Azizi, A. Karlsson, M. Swillo, and B. Jaskorzynska, "Numerical studies of mode gaps and coupling efficiency for line-defect waveguides in two-dimensional photonic crystals," *Phys. Rev. B*, Vol. 64, 155113–155117, 2001.
9. Monat, C., B. Corcoran, D. Pudo, M. Ebnali-Heidari, C. Grillet, M. Pelusi, D. Moss, B. Eggleton, T. White, and T. Krauss, "Slow light enhanced nonlinear optics in silicon photonic crystal waveguides," *IEEE Journal of Selected Topics in Quantum Electronics*, Vol. 16, No. 1, 344–356, 2010.
10. Blanco-Redondo, A., C. Husko, D. Eades, Y. Zhang, J. Li, T. Krauss, and B. Eggleton, "Observation of soliton compression in silicon photonic crystals," *Nature Communications*, Vol. 5, 2014.
11. Geniet, F. and J. Leon, "Energy transmission in the forbidden band gap of a nonlinear chain," *Phys. Rev. Lett.*, Vol. 89, 134102–134105, 2002.
12. Khomeriki, R., "Nonlinear bandgap transmission in optical waveguide arrays," *Phys. Rev. Lett.*, Vol. 92, 063905–063908, 2004.
13. Chen, W. and D. L. Mills, "Gap solitons and the nonlinear optical response of superlattices," *Phys. Rev. Lett.*, Vol. 58, 160–163, 1987.
14. Martijn de Sterke, C. and J. E. Sipe, "Envelope-function approach for the electrodynamics of nonlinear periodic structures," *Phys. Rev. A*, Vol. 38, 5149–5165, 1988.
15. Martijn de Sterke, C. and J. E. Sipe, "Coupled modes and the nonlinear Schrödinger equation," *Phys. Rev. A*, Vol. 42, 550–555, 1990.
16. Agrawal, G. P., *Nonlinear Fiber Optics*, Academic Press, New York, 1989.
17. Kivshar, Y. S. and G. P. Agrawal, *Optical Solitons: From Fibers to Photonic Crystals*, Academic Press, San Diego, California, 2003.
18. Akhmediev, N. N. and A. Ankiewicz, *Solitons: Nonlinear Pulses and Beams*, Chapman and Hall, London, 1997.
19. Segev, M., B. Crosignani, A. Yariv, and B. Fischer, "Spatial solitons in photorefractive media," *Phys. Rev. Lett.*, Vol. 68, 923–926, 1992.
20. Christodoulides, D. N. and R. I. Joseph, "Discrete self-focusing in nonlinear arrays of coupled waveguides," *Opt. Lett.*, Vol. 13, 794–796, 1988.
21. Mandelik, D., H. S. Eisenberg, Y. Silberberg, R. Morandotti, and J. S. Aitchinson, "Band-gap structure of waveguide arrays and excitation of Floquet-Bloch solitons," *Phys. Rev. Lett.*, Vol. 90, 053902–053905, 2003.
22. Khomeriki, R. and J. Leon, "Bistable light detectors nonlinear waveguide arrays," *Phys. Rev. Lett.*, Vol. 94, 243902–243905, 2005.
23. Khomeriki, R. and J. Leon, "Driving light pulses with light in two-level media," *Phys. Rev. Lett.*, Vol. 99, 183601–183604, 2007.
24. Christodoulides, D. N. and R. I. Joseph, "Slow Bragg solitons in nonlinear periodic structures," *Phys. Rev. Lett.*, Vol. 62, 1746–1749, 1989.
25. Millar, P., R. M. De La Rue, T. F. Krauss, J. S. Aitchison, N. G. R. Broderick, and D. J. Richardson, "Nonlinear propagation effects in an AlGaAs Bragg grating filter," *Optics Lett.*, Vol. 24, 685–687, 1999.
26. Aceves, A. B. and S. Wabnitz, "Self-induced transparency solitons in nonlinear refractive periodic media," *Phys. Rev. A*, Vol. 141, 37–42, 1989.
27. Conti, C. and S. Trillo, "Bifurcation of gap solitons through catastrophe theory," *Phys. Rev. E*, Vol. 64, 036617, 2001.

28. Krauss, T., "Slow light in photonic crystal waveguides," *J. Phys. D: Appl. Phys.*, Vol. 40, 2666–2670, 2007.
29. Yasumoto, K., V. Jandieri, and Y. Liu, "Coupled-mode formulation of two-parallel photonic crystal waveguides," *Journal of the Optical Society of America A*, Vol. 30, No. 1, 96–101, 2013.
30. Jandieri, V., K. Yasumoto, and J. Pistora, "Coupled-mode analysis of contra-directional coupling between two asymmetric photonic crystals waveguides," *Journal of the Optical Society of America A*, Vol. 31, No. 3, 518–523, 2014.
31. Taniuti, T. and N. Yajima, "Perturbation method for a nonlinear wave modulation," *Journal of Mathematical Physics*, Vol. 10, 1369–1372, 1969.
32. Oikawa, M. and N. Yajima, "A perturbation approach to nonlinear systems. II. Interaction of nonlinear modulated waves," *Journal of the Physical Society of Japan*, Vol. 37, 486–496, 1974.
33. Taflove, A., *Computational Electrodynamics: The Finite-Difference Time-Domain Method*, Artech House, Norwood, 1995.